Research Article BEU Fen Bilimleri Dergisi 15(2): 594-607 (2026) DOI: 10.17798/bitlisfen.1802057

BİTLİS EREN UNIVERSITY
FEN BİLİMLERİ DERGİSİ
ISSN: 2147-3129 / e-ISSN: 2147-3188

FARADAY ROTATION AS A CONTROL PARAMETER FOR POINCARÉ SPHERE POLARIZATION STATES

Mahmud TEKİN [1*], Fatma TAMBAĞ [2], Koray KÖKSAL [3]

[1] *Gaziantep Islamic Science and Technology University, Department of Technical Sciences Vocational, Gaziantep, Türkiye*
[2] *Bitlis Eren University, Department of Physics, Bitlis, Türkiye*
[3] *Gaziantep Islamic Science and Technology University, Faculty of Engineering and Natural Sciences, Gaziantep, Türkiye*
**** Corresponding Author:*** *mahmud.tekin@gibtu.edu.tr*

Article Info

Received: *October 12, 2025*
Revised: *May 11, 2026*
Accepted: *May 11, 2026*

Keywords
Poincaré Sphere,
Faraday Rotation,
Polarization.

ABSTRACT

Vector beams which are described on higher-order Poincaré spheres provide a powerful framework for representing structured light fields whose polarization and spatial phase are inseparably linked. Although such states can be generated by various optical elements, a practical challenge remains in controlling their polarization change during propagation. In this work, we aim to analyze the role of the Faraday rotation angle as a tunable control parameter that couples directly to the azimuthal coordinate of the Poincaré sphere. Through theoretical modeling and visualizations, we show how linear, circular, and elliptical polarizations evolve under varying Faraday angles, highlighting similarities and differences with intrinsic Poincaré sphere rotations. Our results demonstrate that Faraday rotation can serve as an in-line, magnetically tunable actuator for polarization control, offering a compact and non-mechanical alternative to conventional polarization optics. This perspective opens new opportunities for adaptive imaging, optical communication, sensing, and integrated photonic devices where real-time polarization control of vector modes is required.

1. INTRODUCTION

Vectorial light fields, often described on higher-order Poincaré spheres, have become of great important in modern photonics because they are able to combine spatial structure and polarization into a single, tunable platform [1–3]. An example of such a vectorial light field is shown in Figure 1, where the local polarization vectors vary smoothly across the transverse plane while the field intensity remains spatially structured.

This combination of phase and polarization inhomogeneity enables phenomena such as spin–orbit coupling, optical angular momentum exchange, and polarization-based beam shaping, which lie at the heart of many emerging photonic applications.

Unlike well-known uniformly polarized Gaussian beams, these modes exhibit polarization patterns that vary across the transverse plane and change along propagation, enabling a new kind of properties that are not accessible to scalar light [4]. In the last decade, methods for generating and transforming such states have advanced rapidly, relying on interferometric superpositions, q plates and spin–orbit converters, spatial light modulators, metasurfaces, and selective polarization diffractive optics [5, 6]. This technology components now allow routine access to families of vector beams parameterized by the polar and azimuthal coordinates of a Poincaré sphere, where each point corresponds to a unique global polarization composition and spatial phase arrangement.

License: CC BY-NC 4.0

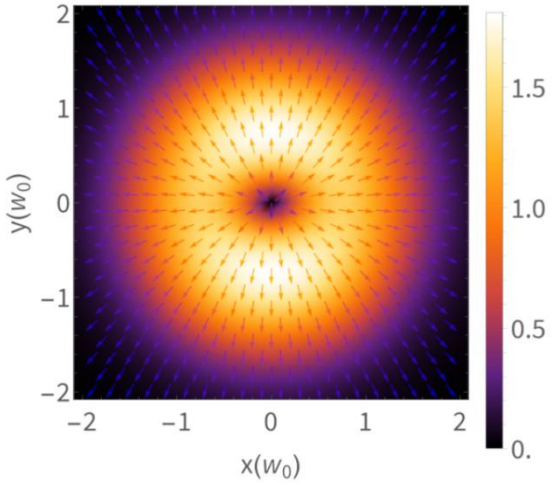


Figure 1. Example of a vectorial light field. The background color map represents the field intensity, while arrows indicate the local polarization direction across the transverse plane. Such spatially varying polarization distributions exemplify the class of structured light fields described on higher-order Poincaré spheres, where spatial and polarization degrees of freedom are intrinsically coupled.

Despite this progress, there remains a practical gap between how these states are prepared and how they are controlled once they are injected into a device or medium. Many photonic platforms require polarization adjustments to be performed in situ after the beam has entered a waveguide, a fiber, a bulk magneto-optic crystal, or a free-space segment inside an instrument [7–9]. Free-space waveplates and static polarization optics are not well suited to that task because they act prior to injection and cannot easily address polarization evolution along the propagation axis. What is needed is a compact material-based mechanism that can modulate the effective Poincaré sphere coordinates of the field while it propagates in the medium, ideally with an externally adjustable control variable.

Magneto-optic materials offer precisely this opportunity. In such media, an applied magnetic field lifts the degeneracy between left- and right-handed circular polarization components, producing a differential phase and, consequently, a rotation of linear polarization, an effect historically known as Faraday rotation [10–12]. In practice, the Faraday rotation provides a continuous and reversible means of controlling the polarization state through external magnetic or electric fields, without disturbing the optical setup. Although Faraday rotation has long been exploited for optical isolation and magnetic sensing, its role as a systematic control parameter for higher-order Poincaré modes has not been mapped comprehensively. Most existing analyses treat magneto-optic effects for uniform polarizations or focus on scalar phase modulation, leaving open how the Faraday angle couples to the Poincaré sphere angles that define the polarization composition and spatial structure of vector beams [13].

This coupling is significant for two main reasons. First, on the Poincaré sphere, the polar angle defines the relative amplitudes of the left- and right-handed circular polarization components, while the azimuthal angle determines their relative phase. Consequently, any physical process that selectively advances the phase of one circular component with respect to the other as occurs in magneto-optic media causes the polarization state to trace a path along lines of constant latitude on the sphere. In physical terms, this corresponds to a continuous rotation of the polarization orientation while maintaining a fixed ellipticity. The Faraday angle is, by construction, an externally tunable relative phase between those circular bases, and therefore it should act as a direct handle on the azimuthal coordinate of the Poincaré sphere. Second, when the underlying spatial modes are structured, polarization rotation does not merely "spin" a uniform vector; it changes the local polarization map across the beam and its evolution along the propagation direction. Being able to tune that evolution with a single scalar control parameter is highly attractive for photonic systems design.

A controlled interplay between Poincaré angles and Faraday rotation has immediate implications for polarization-sensitive imaging and microscopy. Techniques such as polarization-encoded contrast enhancement, differential interference, and vectorial point-spread engineering benefit when the incident

polarization can be swept through a set of states without moving optics. By tuning the Faraday angle, one can program a sequence of polarization states delivered to the focal plane or specimen with sub-millisecond response set by magnetic driver electronics rather than by mechanical rotation stages. This capability reduces alignment sensitivity and enables compact polarization scanners for endoscopy, optical coherence tomography, and confocal systems where moving elements are undesirable.

Communication and information processing stand to benefit as well. Polarization is a natural degree of freedom for multiplexing channels and for implementing mode-division schemes in both free space and guided platforms. In vector-mode links, robustness depends on the ability to compensate drifts that scramble polarization states along the path. A magneto-optic section that maps Faraday angle to Poincaré-azimuth offers adaptive compensation without inserting additional interferometric hardware. Similarly, in integrated photonics, garneton-silicon or other magneto-optic overlays can be patterned to act as polarization controllers that re-bias vector modes at key nodes of a circuit, complementing phase shifters and mode converters already in use [14–17].

Sensing is another natural application domain. Faraday rotation is widely used to measure magnetic fields, but its action on vector beams opens alternative observables beyond a single rotation angle. Because polarization patterns in vector beams are spatially non-uniform, a uniform change in the relative circular phase imprints a distinctive, global deformation on those patterns as they propagate. Imaging that deformation can, in principle, enhance dynamic range and immunity to local defects, providing distributed sensing of magnetic fields or magneto-optic coefficients over extended apertures. Conversely, known magneto-optic responses can be used to "write" specific polarization evolution, which can serve as calibration targets for complex optical systems [18].

From a device-engineering viewpoint, the Faraday angle is appealing because it is continuous, reversible, and compatible with standard actuation schemes. Magnetic bias can be supplied by permanent magnets for static operation, by coils for dynamic control, or even by integrated current lines in on-chip implementations. The same physics can be realized across a broad spectral range by choosing appropriate magneto-optic media, from visible iron garnets to near-infrared ceramics and chalcogenides. This breadth means the same control concept can be translated from table-top free-space experiments to fiber components and integrated photonics without changing the underlying modeling framework [19].

While several studies have characterized how vector beams transform under static birefringence, spatially varying retarders, and geometric-phase elements, fewer works have isolated the specific role of Faraday rotation as an effective Poincaré-azimuth control for the propagation of polarization vectors [1, 13, 20]. The novelty of this work is because of that Faraday rotation is not merely an additional polarization rotation mechanism, but a controllable and propagation-dependent azimuthal degree of freedom on the Poincaré sphere. In part, this is because vector beams involve a proliferation of parameters: spatial mode indices, beam size and divergence, focusing conditions that introduce longitudinal fields, and material anisotropies. It is therefore valuable to separate these effects and highlight a clean, experimentally accessible relationship: how a tunable Faraday angle, applied along the propagation axis, systematically reorganizes the polarization vectors of linear, circular, and elliptical states as they advance.

The present work addresses that need by assembling a model and a set of clear visualizations that link the Faraday angle to the Poincaré-sphere description. Our objective is not to exhaust the taxonomy of vector beams but to provide an operational picture that practitioners can apply immediately: given a chosen point on the Poincaré sphere, how will the polarization vectors evolve in space when a magneto-optic section of known rotation is inserted? By framing the outcome in terms of recognizable trajectories and cross-sections, we aim to make the effect legible to experimentalists who must decide how much magnetic bias to apply and where to place a magneto-optic element in an optical train.

A useful takeaway that emerges from our analysis is a set of expectations across canonical polarization families. For linearly polarized inputs, the Faraday angle replicates the action of sweeping the Poincaré azimuth, producing a clean rotation of the polarization direction that remains uniform across the beam in the paraxial regime. For elliptically polarized inputs, the same control interpolates smoothly between linear and circular features, yielding predictable changes in the polarization map. For circularly polarized inputs, the Faraday angle introduces a relative phase that does not invert handedness; instead,

it shifts the internal phase reference without crossing hemispheres on the Poincaré sphere. These regimes align with intuitive, lab-ready observations and provide a checklist for diagnosing magneto-optic behavior in complex optical setups.

The broader significance of this perspective is that it elevates the Faraday angle from a scalar "rotation readout" to a genuine state-engineering parameter for vector light. In practice, that means magneto-optic sections can be treated as programmable Poincaré-azimuth actuators that operate in line with the beam, complementing static polarization optics and geometric-phase devices. Because the actuation is electrical or magnetic rather than mechanical, it lends itself to feedback control, rapid modulation, and monolithic integration. These features are increasingly important in applications where polarization must be adjusted on the fly adaptive microscopes, reconfigurable laser processing, secure links that scramble polarization states, and instrument calibration workflows that need reproducible trajectories on the Poincaré sphere.

As we mentioned previously, the structured vectorial light fields can be elegantly represented on the Poincaré sphere, which geometrically encodes all possible polarization states. In this representation, the polar coordinate Θ_P defines the relative weighting of the right- and left circular components, and the azimuthal coordinate Φ_P sets their relative phase. Figure 2 illustrates the conventional first-order Poincaré sphere and the position of canonical polarization states. This geometric picture will serve as the foundation for the theoretical formulation developed in the next section, where magneto-optic Faraday rotation is shown to correspond to azimuthal motion on the sphere.

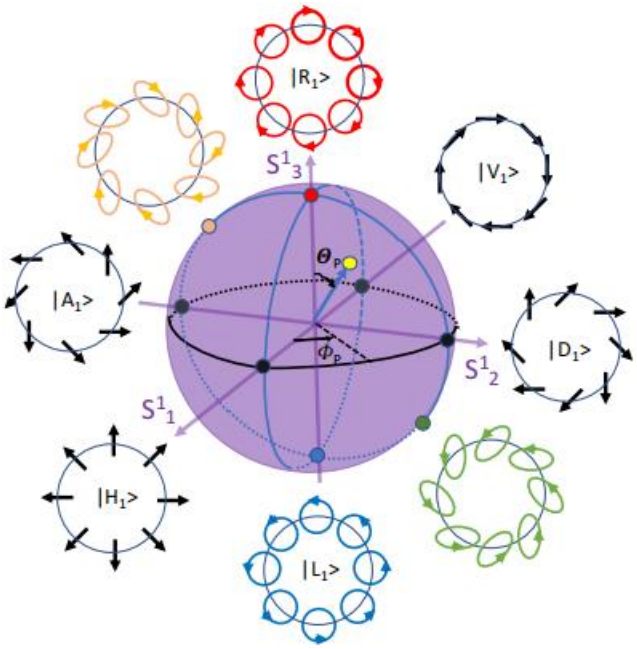


Figure 2. First-order Poincaré sphere in the classical optical convention. Each point corresponds to a distinct polarization state characterized by polar angle Θ_P and azimuth Φ_P. Linear polarizations reside on the equator, while right- and lefthanded circular polarizations occupy the poles. Intermediate points correspond to elliptically polarized states. This representation provides the geometric foundation for linking Faraday rotation to azimuthal evolution on the Poincaré sphere.

In summary, the field has developed an impressive toolkit for creating vector beams, yet a simple and tunable means of steering their polarization evolution during propagation has been under-articulated. Faraday rotation provides exactly such a lever. By articulating its connection to the Poincaré-sphere angles and illustrating the consequences for linear, circular, and elliptical inputs, this work provides a compact framework that can be translated across platforms from free-space optics to fibers and integrated devices—where controlled polarization dynamics are both scientifically revealing and technologically enabling.

2. THEORY

The theoretical description of vectorial structured light fields requires a formulation that accounts simultaneously for spatial phase, polarization state, and propagation dynamics. In the paraxial approximation, where the beam propagates primarily along the positive z-direction, a convenient starting point is the vector potential representation in cylindrical coordinates r = (ρ, ϕ, z). We express the optical field as,

$$\mathrm{A(r)} = \hat{\epsilon}_\ell \tilde{\mathcal{F}}_{\ell,p}(\rho, z) e^{ik_z z} \tag{1}$$

where $\tilde{\mathcal{F}}_{\ell,p}(\rho, z)$ describes the radial profile of the vortex beam (which can be taken as Laguerre–Gaussian type in the general case), and is the longitudinal wavevector. The essential polarization structure is carried by, which encodes a higher-order Poincaré sphere state.

The polarization vector $\hat{\epsilon}_\ell$is written as a superposition of left- and right-circular polarization states, each carrying opposite helical phase factors:

$$\hat{\epsilon}_\ell = e^{i\ell\phi} \frac{(\hat{\boldsymbol{x}} - i\hat{\boldsymbol{y}})}{\sqrt{2}} \sin\left(\frac{\Theta_P}{2}\right) e^{i\Phi_P/2} + e^{-i\ell\phi} \frac{(\hat{\boldsymbol{x}} + i\hat{\boldsymbol{y}})}{\sqrt{2}} \cos\left(\frac{\Theta_P}{2}\right) e^{-i\Phi_P/2} \tag{2}$$

where (Θ_P, Φ_P) are spherical coordinates on the Poincaré sphere. The polar angle Θ_P controls the relative weights of the circular components, while the azimuth Φ_P determines their relative phase. This construction generalizes the familiar Bloch-sphere representation of polarization to higher-order vector modes with topological charge ℓ.

It is often convenient to introduce the complex Poincaré functions,

$$\mathcal{U}_\mathcal{P} = \frac{1}{\sqrt{2}} \sin\left(\frac{\Theta_P}{2}\right) e^{i\Phi_P/2}$$

$$\mathcal{V}_\mathcal{P} = \frac{1}{\sqrt{2}} \cos\left(\frac{\Theta_P}{2}\right) e^{-i\Phi_P/2} \tag{3}$$

so that Eq. (2) can be compactly expressed as,

$$\hat{\epsilon}_\ell = e^{i\ell\phi}(\hat{x} - i\hat{y})\mathcal{U}_\mathcal{P} + e^{-i\ell\phi}(\hat{x} + i\hat{y})\mathcal{V}_\mathcal{P} \tag{4}$$

which can be inserted into Eq. (1) yielding the general vector potential,

$$A(r) = \left[(\hat{x} - i\hat{y})e^{i\ell\phi}\mathcal{U}_\mathcal{P} + (\hat{x} + i\hat{y})e^{-i\ell\phi}\mathcal{V}_\mathcal{P}\right] \tilde{\mathcal{F}}_{\ell,p}(\rho, z) e^{ik_z z} \tag{5}$$

When the beam propagates inside a magneto-optic medium under a longitudinal magnetic field, the left- and right-circular components acquire different refractive indices, $n-$ and $n+$. Thus, the two contributions to the vector potential must be written separately such that,

$$A = A_1 + A_2 \tag{6}$$

with

$$A_1 = (\hat{x} - i\hat{y})\, \mathcal{F}^{(1)}_{\ell,\mathcal{P}}(r) e^{in_- k_z z}$$

$$A_2 = (\hat{x} + i\hat{y})\, \mathcal{F}^{(2)}_{\ell,\mathcal{P}}(r) e^{in_+ k_z z} \tag{7}$$

where

$$\mathcal{F}_{\ell,\mathcal{P}}^{(1)}(r) = \mathcal{U}_{\mathcal{P}} e^{i\ell\phi} \tilde{\mathcal{F}}_{\ell,p}(\rho)$$

$$\mathcal{F}_{\ell,\mathcal{P}}^{(2)}(r) = \mathcal{V}_{\mathcal{P}} e^{-i\ell\phi} \tilde{\mathcal{F}}_{\ell,p}(\rho) \tag{8}$$

Now, we can write the refractive indices as $n\pm = \eta \pm \Delta n$ and introduce the Faraday angle $\theta = k_z L \Delta n$, so that the exponential factors can be recast as,

$$e^{in_{\pm}k_z z} = e^{ik_z z\eta} e^{\pm i\theta} \tag{9}$$

which shows that the medium induces an additional relative phase of $\pm\theta$ between the two circular polarization components. This phase has the same functional role as the Poincaré azimuth Φ_P, establishing the equivalence between magneto-optic rotation and azimuthal motion on the Poincaré sphere.

The corresponding electric and magnetic fields are obtained from Maxwell's curl equations:

$$B = \nabla \times A \, , E = i\omega A \tag{10}$$

Carrying out the differentiation leads to explicit transverse and longitudinal components. For the first contribution, one obtains,

$$E_1 = i\omega(\hat{x} - i\hat{y})\mathcal{F}^{(1)} e^{in_- k_z z} - \hat{z}c\left(\frac{\partial \mathcal{F}^{(1)}}{\partial x} - i\frac{\partial \mathcal{F}^{(1)}}{\partial y}\right) e^{in_- k_z z}$$

$$B_1 = i\frac{\omega}{c}(\hat{y} + i\hat{x})\mathcal{F}^{(1)} e^{in_- k_z z} - \hat{z}\left(i\frac{\partial \mathcal{F}^{(1)}}{\partial x} + \frac{\partial \mathcal{F}^{(1)}}{\partial y}\right) e^{in_- k_z z} \tag{11}$$

Similarly, for the second component,

$$E_2 = i\omega(\hat{x} + i\hat{y})\mathcal{F}^{(2)} e^{in_+ k_z z} - \hat{z}c\left(\frac{\partial \mathcal{F}^{(2)}}{\partial x} + i\frac{\partial \mathcal{F}^{(2)}}{\partial y}\right) e^{in_+ k_z z}$$

$$B_2 = i\frac{\omega}{c}(\hat{y} - i\hat{x})\mathcal{F}^{(2)} e^{in_+ k_z z} + \hat{z}\left(i\frac{\partial \mathcal{F}^{(2)}}{\partial x} - \frac{\partial \mathcal{F}^{(2)}}{\partial y}\right) e^{in_+ k_z z} \tag{12}$$

The total fields are given, $E = E_1 + E_2, B = B_1 + B_2$.

These expressions demonstrate how both transverse and longitudinal field components acquire Faraday dependent phase factors, which rotate the effective polarization vector along the propagation direction.

The theoretical framework developed in this section establishes how vectorial structured light evolves in magneto-optic media by unifying spatial, polarization, and propagation degrees of freedom within a single analytical formulation. Starting from the vector potential in cylindrical coordinates, the beam is described as a coherent superposition of counter-rotating circular polarization components, each carrying an opposite helical phase factor. This representation naturally maps onto the higher-order Poincaré sphere, where the polar coordinate $\Theta_P$determines the amplitude balance between left-and right-handed circular modes, and the azimuth $\Phi_P$defines their relative phase.

When a longitudinal magnetic field is applied, the magneto-optic medium lifts the degeneracy between these two components by introducing distinct refractive indices $n\pm = \eta \pm \Delta n$. The resulting phase difference, $2\theta = 2k_z L \Delta n$, manifests as a Faraday rotation, which acts as a controllable shift of the Poincaré azimuth. Hence, the Faraday angle and $\Phi_P$are mathematically equivalent parameters governing the evolution of polarization states on the sphere.

The explicit electric and magnetic field expressions derived from Maxwell's curl equations reveal that both the transverse and longitudinal components inherit this magnetically tunable phase. The theory therefore demonstrates that a Faraday-induced birefringence not only rotates the overall polarization vector but also modulates the internal vectorial texture of the field. In essence, Faraday rotation emerges as an external control parameter for navigating polarization trajectories on the higher order Poincaré sphere, providing a rigorous foundation for magnetically tunable vector-beam generation, modulation, and propagation in free-space and integrated photonic systems.

For $\Theta_P = \pi/2$ and $\ell = 0$, the two circular components have equal amplitude, producing a linearly polarized state in the *xy* plane. Varying the Poincaré azimuth Φ_P from *0* to 2π then results in a uniform rotation of the polarization direction, corresponding to motion along the equator of the Poincaré sphere. The same physical effect arises when Φ_P is held fixed and the Faraday angle θ is swept through an equivalent range, confirming the functional equivalence between θ and Φ_P. This correspondence forms the conceptual basis of Figures 3 and 4, which depict linear polarization rotation under geometric and magneto-optic control, respectively.

For $\Theta_P = 0$ or π, only one circular component contributes, yielding purely right- or left-handed circular polarization. In this limit, varying θ introduces an additional phase factor $e^{\pm i\theta}$ but leaves the handedness unchanged, in agreement with the results illustrated in Figure 5. This observation highlights a fundamental constraint of Faraday rotation: while it alters the relative phase between spin components, it cannot invert helicity.

Intermediate values of Θ_P produce elliptically polarized states where the two circular components contribute unequally. In this regime, the Faraday angle continuously modifies the relative phase, leading to a progressive rotation of the polarization ellipse along the propagation direction. This gradual deformation is visualized in Figure 6, where the ellipse orientation and eccentricity evolve as a function of θ, demonstrating how magnetic control enables smooth transitions between circular, elliptical, and linear polarization states.

The derivation presented above shows that the Faraday angle θ explicitly enters the exponential propagation factors of the two circular components and therefore acts as an externally tunable azimuthal parameter on the Poincaré sphere. The complete field solutions in Eqs. (11), (12) quantitatively describe how θ governs the evolution of the polarization vector for any combination of (Θ_P, Φ_P, ℓ). This theoretical framework thus provides the analytical foundation for the visualizations presented in the Results section, bridging magneto-optic phase dynamics and the geometric representation of polarization on the Poincaré sphere.

3. RESULTS

The theoretical framework developed above establishes a direct connection between magneto-optic phase accumulation and the azimuthal evolution of vectorial polarization states on the Poincaré sphere. In this section, we present numerical and graphical results that illustrate how this coupling manifests in structured beams. Four representative cases are discussed, each emphasizing a distinct physical aspect of the Faraday-induced modulation: (i) the longitudinal evolution of the polarization ellipse, (ii) the azimuthal redistribution of vector components, (iii) the magnetically driven deformation of polarization topology, and (iv) the correlation between the Faraday angle and the spatially varying polarization pattern. Together, these figures demonstrate how magnetic control can serve as a practical mechanism for tuning the internal structure of vector beams in real space.

Figure 3 shows the evolution of the polarization ellipse along propagation for different Poincaré azimuths. Each colored lobe represents the local polarization ellipse of the optical field as it propagates in the $+z$ direction under a uniform longitudinal magnetic field. The calculation assumes a paraxial vector beam with equal circular components at the input, corresponding to a linearly polarized state on the equator of the Poincaré sphere.

The color map encodes successive increments of Φ_P from *0* to 2π, illustrating how a uniform Faraday rotation produces a spatially periodic modulation of the polarization direction without altering the intensity profile of the beam. The result is a helicoidal polarization texture, where the orientation of the

polarization vector precesses around the propagation axis. This figure captures the essence of magnetically controlled azimuthal evolution: the Faraday rotation acts as a dynamic phase dial, steering the polarization trajectory along lines of constant latitude on the Poincaré sphere. The clear periodicity of the ellipses along the z axis confirms the equivalence between the optical Faraday effect and an externally tunable azimuthal modulation of vectorial structured light.

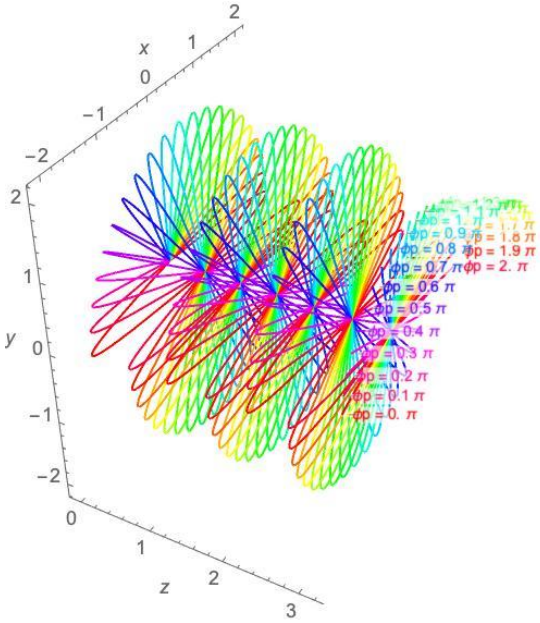


Figure 3. The figure illustrates the longitudinal evolution of the polarization ellipse of a vector beam propagating through a magneto-optic medium. At each position z, the local polarization state is plotted as an ellipse, showing that a differential phase between the left- and right-circular components induces a continuous rotation of the polarization direction along the propagation axis. A differential phase between the left- and right-circular components, induced by the Faraday angle θ, continuously rotates the local polarization direction along z. The color progression from red to cyan corresponds to increasing Poincaré azimuth Φ_P, revealing a helical polarization texture where the orientation of the polarization vector precesses around the propagation axis. This confirms that Faraday rotation acts as a tunable azimuthal control on the Poincaré sphere.

Figure 4 shows the continuation of the polarization evolution when the Faraday angle θ is varied systematically from 0 to π. Compared to Figure 3, where the azimuthal parameter $\Phi_P$was externally defined, the present case demonstrates how the same rotational behavior naturally emerges from magneto-optic phase accumulation inside the medium. As θ increases, the relative phase between left- and right-circular components changes continuously, causing the polarization ellipses to precess with a rate determined by the magnetic bias. The polarization structure therefore exhibits a periodic helicoidal texture along the z axis, confirming that the Faraday angle functions as an intrinsic tuning knob for azimuthal polarization control. The correspondence between θ and $\Phi_P$highlights the physical equivalence between magnetic field–induced birefringence and azimuthal evolution on the Poincaré sphere.

The theoretical framework developed in this study aims to bridge the gap between magneto-optic physics and the modern field of structured light. Traditional descriptions of the Faraday effect treat it primarily as a scalar rotation of linear polarization, typically used in isolation, sensing, or modulation devices. However, when light carries spatially varying polarization and phase as in vector or vortex beams—the same interaction acquires a far more intricate character. In such fields, polarization varies across the transverse plane, and any magnetooptic phase accumulation acts locally on that distribution. This behavior is illustrated in Figure 3 by mapping how the polarization ellipses evolve when the Poincaré azimuth Φ_P is varied systematically, establishing a direct visual link between azimuthal motion on the Poincaré sphere and spatial polarization rotation in real space.

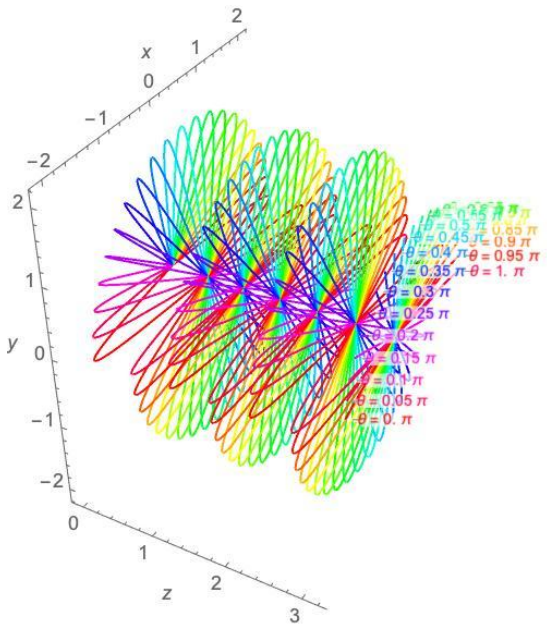


Figure 4. Polarization precession as a function of the Faraday angle. At each position zzz, the local polarization state is plotted as an ellipse, showing that a differential phase between the left- and right-circular components induces a continuous rotation of the polarization direction along the propagation axis. For increasing values of θ (from 0 to π), the polarization ellipses undergo a continuous azimuthal rotation analogous to that in Figure 3. Here, the rotation originates directly from the magneto-optic phase difference rather than a predefined Poincaré azimuth. The comparison between the two figures confirms that the Faraday angle and Φ_P play equivalent roles in governing polarization evolution along the propagation axis.

This correspondence becomes physically grounded in the magneto-optic domain, as demonstrated by the Faraday-controlled case shown in Figure 4. Here, the same rotational pattern emerges, but now driven by the Faraday angle θ, which encodes the differential phase between left- and right-circular components. The equivalence between these two representations one geometric, the other magnetically induced constitutes the central theoretical insight of this work. It shows that the Faraday effect can serve as a continuous and reversible control parameter for polarization evolution, playing the same functional role as geometric-phase modulation but with all-electronic tunability and without any mechanical or interferometric elements.

This finding carries significant implications for photonic system design. The ability to manipulate the internal polarization structure dynamically through a magnetic field enables compact, robust, and broadband control of vector beams. Because the Faraday angle scales linearly with both magnetic field strength and material Verdet constant, the same principle can be implemented across diverse spectral regions from visible to near infrared by selecting appropriate magneto-optic media. Thus, the transition from Figure 3 to Figure 4 symbolically captures a shift from passive geometric rotation to actively tunable magnetic control, bridging fundamental optical geometry with applied photonics.

Beyond modulation, the sensitivity of polarization textures to small variations in the Faraday angle suggests promising sensing and metrological applications. A uniform magnetic bias imposes a predictable deformation of the polarization field, which can be imaged to infer spatial variations in magnetic field strength or magneto-optic coefficients. Conversely, known magneto-optic responses can be used to generate calibrated polarization evolution that serve as test patterns for polarization sensitive microscopy and optical coherence tomography. The principle demonstrated by Figure 3 and Figure 4 thus extends naturally to magnetically controlled polarization scanning and distributed field mapping.

At a conceptual level, these results motivate a unified perspective in which magnetic field control and structured light physics converge on the same geometric foundation. The Faraday effect, long regarded as a simple rotation of linear polarization, emerges here as a topological actuator capable of steering the

polarization state across the Poincaré sphere with precision. By linking an experimentally accessible scalar parameter the Faraday angle to the spatial geometry of polarization, this study reveals a new paradigm for magnetically programmable photonics, where spin, orbital, and magnetic degrees of freedom interact coherently to shape the evolution of light.

Figure 5 provides an extended visualization of the magnetically driven evolution of circular polarization components. In contrast to Figure 3 and Figure 4, which focused on the azimuthal rotation of the polarization ellipse for linearly polarized vector modes, this figure isolates the dynamics of the individual circular components that form the basis of those vector states. Each helical trajectory corresponds to a constant-amplitude circularly polarized component whose optical axis precesses as the Faraday angle θ increases from 0 to π. The left panels depict the three dimensional helical evolution along the propagation axis, whereas the right panels present top-view projections, revealing the circular loci traced by the field vectors in the transverse plane. The gradual transition of colors from red ($\theta = 0$) to green ($\theta = \pi$) illustrates the continuous magnetic tuning of the polarization phase.

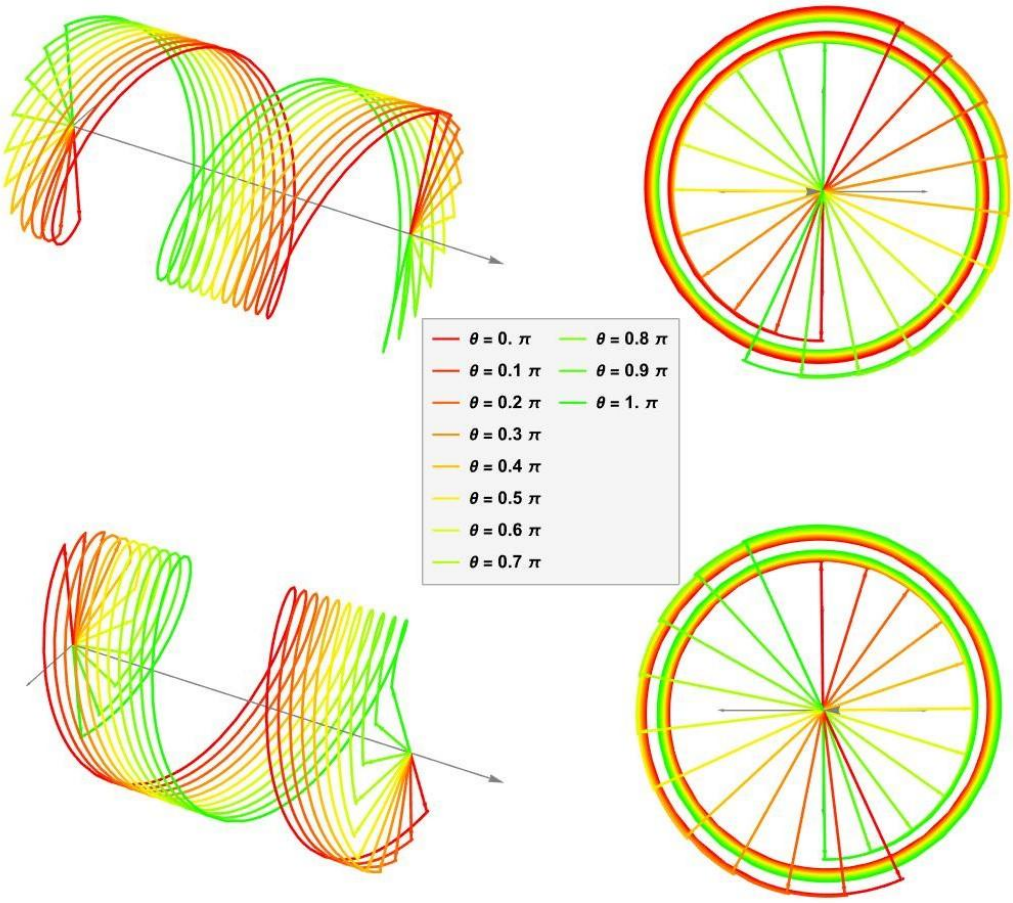


Figure 5. Helical evolution of circular polarization components under Faraday rotation. The figure compares the two counter rotating circular components composing a vector beam as the Faraday angle θ increases from 0 to π. The left panels show the three-dimensional helical evolution of each component along z, while the right panels display their top-view projections in the transverse plane. The smooth color gradient from red to green encodes the magnetic tuning of phase, demonstrating that the two components undergo equal but opposite precession. This visualization emphasizes that Faraday rotation introduces a geometrical coupling between optical spin and propagation, turning polarization evolution into a magnetically controlled helical motion in real space.

The upper and lower rows represent the two counter rotating circular components, $(\hat{\boldsymbol{x}}-i\hat{\boldsymbol{y}})$ and $(\hat{\boldsymbol{x}}+i\hat{\boldsymbol{y}})$, which acquire opposite phase shifts of $\pm\theta$ as they propagate through the magneto-optic medium. As the magnetic bias increases, the relative phase difference between these components produces a helical twisting of their polarization vectors. The comparison between the two rows clearly reveals their

opposite sense of rotation one right-handed, the other left-handed reflecting the fundamental symmetry breaking introduced by the Faraday effect. These plots highlight the geometric nature of magneto-optic rotation: rather than acting as a simple planar rotation of the polarization ellipse, it generates a full three-dimensional precession of the field vector, transforming the polarization basis itself. This geometric visualization confirms that Faraday rotation serves as an adjustable topological coupling between the spin and propagation degrees of freedom of light, opening pathways for dynamic control of vector-beam helicity and structured light in magnetically responsive photonic systems.

The final set of simulations explores the intermediate regime between purely circular and purely linear polarization, where the optical field exhibits an intrinsic ellipticity. In this configuration, the two circular components contributing to the field have unequal amplitudes, resulting in an elliptical polarization vector whose orientation and shape evolve simultaneously under the influence of the Faraday effect. This regime represents the most general case of magneto-optic modulation, in which both the relative phase and the amplitude ratio of the circular components vary with the applied magnetic bias. Unlike the symmetric behavior of the purely circular or linear cases, the evolution of an elliptically polarized state introduces an additional geometric degree of freedom: the rotation of the polarization ellipse's major axis and the modulation of its eccentricity along propagation.

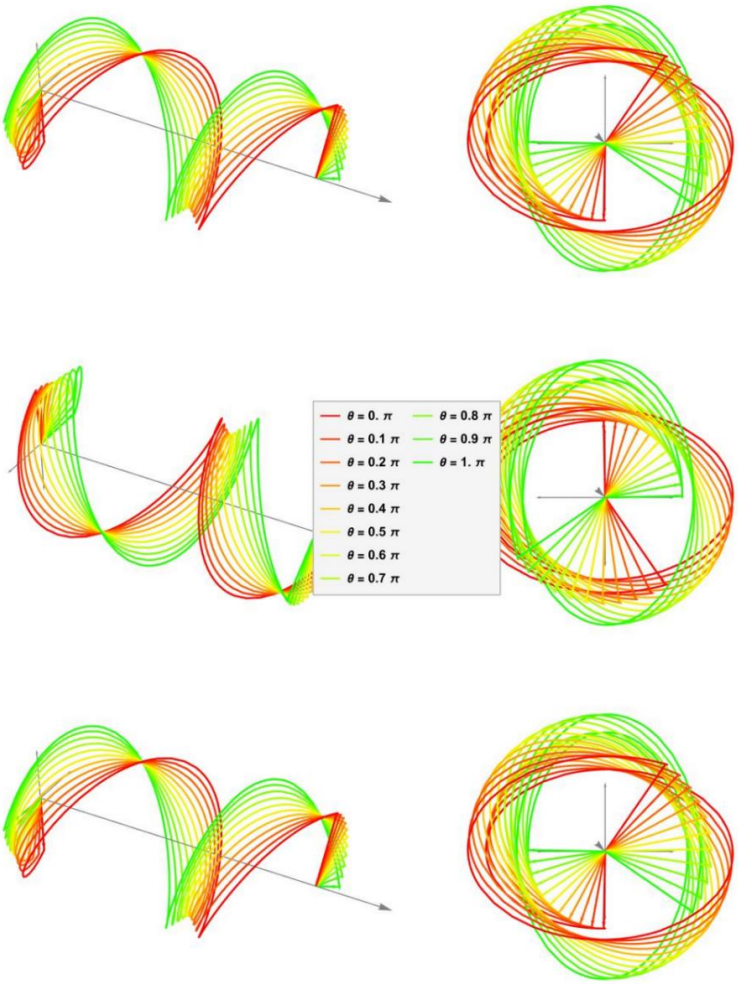


Figure 6. Evolution of elliptically polarized light under Faraday rotation. The figure shows the spatial evolution of elliptically polarized states as the Faraday angle θ increases from 0 to π. The left panels depict three-dimensional helices traced by the polarization vector, while the right panels present transverse-plane projections illustrating the periodic modulation of ellipticity. The gradual color transition from red to green encodes increasing θ, showing that the magnetic field simultaneously rotates and reshapes the polarization ellipse, bridging circular and linear regimes through continuous magneto-optic tuning.

The three-dimensional helices on the left side of Figure 6 depict how the electric-field vector precesses for increasing values of the Faraday angle θ, ranging from 0 to π. As the magnetic field increases, the polarization trajectory becomes progressively tilted and stretched, reflecting the coupling between phase accumulation and amplitude imbalance of the two spin components. The corresponding transverse-plane projections on the right reveal that the polarization traces no longer form perfect circles as in the circularly polarized case but closed ellipses whose eccentricity oscillates periodically with θ. This indicates that the magneto-optic interaction not only rotates the polarization vector but also modulates its ellipticity, providing dual control over both azimuth and elliptic phase.

A key implication of this behavior is that the Faraday effect can continuously transform any polarization state on the Poincaré sphere by sweeping the optical field along a non-equatorial trajectory. Such trajectories represent controlled transitions between right- and left-handed elliptic states, traversing intermediate linear polarization points in a cyclic manner. From a geometric perspective, this corresponds to following constant-latitude circles on the Poincaré sphere that shift in elevation as θ changes, effectively enabling three-dimensional polarization sculpting via magnetic tuning. This tunability demonstrates that the Faraday angle acts as a generalized coordinate governing both the orientation and shape of polarization states.

The elliptical regime also has practical consequences for optical communication and imaging systems. In mode-division multiplexing, elliptical polarization modes can be more resilient to birefringence and alignment errors than strictly linear or circular states. Being able to dynamically re-bias these modes through a magneto-optic section allows adaptive compensation for polarization drifts in fibers and integrated circuits. Similarly, in polarization-resolved microscopy, magnetically controlled ellipticity could be used to probe material anisotropies by sweeping the polarization eccentricity across specific orientations, enhancing contrast and selectivity without mechanical components.

In summary, the results presented in Figure 6 reveal the most general manifestation of magneto-optic coupling in structured light. They show that a uniform magnetic field does not merely rotate the polarization direction it reshapes the polarization topology itself. The Faraday angle thus emerges as a unified control parameter capable of continuously navigating between circular, elliptical, and linear regimes, making it a powerful tool for programmable polarization engineering across diverse photonic platforms.

4. CONCLUSION

This study establishes a unified theoretical framework linking magneto-optic Faraday rotation to the geometric structure of the Poincaré sphere for vectorial light fields. By decomposing the optical field into circular polarization components and tracking their phase evolution under a magnetic bias, we have shown that the Faraday angle θ functions as a tunable azimuthal coordinate controlling the orientation and shape of the polarization vector. The analytical formulation and subsequent visualizations demonstrate that magneto-optic interactions can be interpreted not merely as scalar polarization rotations but as geometric transformations within the higher-order Poincaré space of structured light. This reinterpretation expands the traditional understanding of the Faraday effect into a multidimensional phenomenon coupling spin, phase, and spatial degrees of freedom.

A key result is the demonstration that the Faraday angle and the Poincar´e azimuth Φ_P are functionally equivalent in governing polarization evolution. This equivalence was illustrated for linear, circular, and elliptical states, showing how magnetic-field–induced birefringence maps directly onto the geometry of the Poincaré sphere. Such correspondence offers a practical means of translating magnetic field control into precise polarization engineering. In this sense, the Faraday effect can be regarded as a geometric control mechanism for light, enabling continuous and reversible polarization manipulation without the need for moving parts, interferometric assemblies, or electro-optic crystals.

Beyond its theoretical significance, the framework developed here lays the groundwork for a new class of magnetically programmable photonic systems. Because Faraday rotation is broadband and material-dependent, the same physical principle can be implemented from the visible to the near-infrared range by choosing appropriate magneto-optic media such as iron garnets, yttrium iron oxides, or chalcogenides. In integrated photonic platforms, the concept translates naturally into on-chip magnetic

tuning via patterned garnet films or current driven microcoils, allowing real-time reconfiguration of polarization states and vector modes. This opens a path toward compact polarization controllers, beam shapers, and adaptive isolators in both free-space and guided-wave optics.

The insights presented here also have strong implications for sensing and metrology. Because the polarization structure of vector beams is highly sensitive to magneto-optic phase shifts, imaging the resulting polarization deformation can yield distributed information about local magnetic fields or magneto-optic constants. Conversely, well-characterized Faraday responses can be used as reference standards for calibrating polarization-sensitive instruments or as test fields for verifying numerical polarization models. In this dual role, the Faraday effect emerges as both a diagnostic and an actuation mechanism, allowing light itself to probe and respond to magnetic environments with intrinsic spatial resolution.

Looking forward, the geometrical perspective introduced in this work suggests new opportunities in magnetically controlled topological photonics, optical communication, and quantum light modulation. Combining Faraday-tuned vector beams with structured materials, metasurfaces, or spin-orbit converters could enable hybrid systems where polarization, phase, and orbital angular momentum are simultaneously governed by magnetic bias. Such approaches would make it possible to design all-magnetic logic elements, nonreciprocal light routers, and quantum-state encoders that rely on Faraday rotation as a fundamental resource rather than a secondary effect. By reinterpreting a century-old phenomenon through the language of modern structured optics, this work positions magneto-optic coupling as a key enabler of the next generation of adaptive and topological photonic technologies.

Conflict of Interest Statement

There is no conflict of interest between the authors.

Statement of Research and Publication Ethics

The study is complied with research and publication ethics.

Artificial Intelligence (AI) Contribution Statement

The authors declare that this manuscript was written and analyzed by the authors. Language editing assistance was used; however, the scientific content, data analysis, and figures are entirely the authors' own work.

Contributions of the Authors

The experiments were performed by M. Tekin, and image processing was carried out by F. Tambağ. Conceptualization and methodology were developed and refined by K. Köksal. All authors contributed to the analysis and writing of the manuscript.

REFERENCES

[1] G. Milione, H. I. Sztul, D. A. Nolan, and R. R. Alfano, *Higher-Order Poincaré Sphere, Stokes Parameters, and the Angular Momentum of Light*, Phys. Rev. Lett. 107, 053601, 2011.

[2] Y. Liu, X. Ling, X. Yi, X. Zhou, H. Luo, and S. Wen, *Realization of Polarization Evolution on Higher-Order Poincaré Sphere with Metasurface*, Appl. Phys. Lett. 104, 191110, 2014.

[3] R. Fickler, L. Kopf, and M. Ornigotti, *Higher-Order Poincaré Spheres and Spatiospectral Poincaré Beams*, Phys. Rev. Research 6, 033298, 2024.

[4] M. McLaren, T. Konrad, M. Agnew, J. Leach, and A. Forbes, *Measuring the Nonseparability of Vector Vortex Beams*, Phys. Rev. A 92, 023833, 2015.

[5] L. Marrucci, C. Manzo, and D. Paparo, *Optical Spin-to-Orbital Angular Momentum Conversion in Inhomogeneous Anisotropic Media*, Phys. Rev. Lett. 96, 163905, 2006.

[6] H. Rubinsztein-Dunlop, A. Forbes, M. V. Berry, M. R. Dennis, D. L. Andrews, M. Mansuripur, and et al., *Roadmap on Structured Light*, J. Opt. 19, 013001, 2017.

[7] F. Lei, G. Tkachenko, J. M. Ward, and S. N. Chormaic, *Complete Polarization Control for a Nanofiber Waveguide Using Directional Coupling*, Phys. Rev. Applied 11, 064041, 2019.

[8] W. Xiong, C. W. Hsu, Y. Bromberg, J. E. Antonio-Lopez, R. A. Correa, and H. Cao, *Complete Polarization Control in Multimode Fibers with Polarization and Mode Coupling*, Light: Science&Applications 7, 2018.

[9] A. E. Kaplan, V. Vitali, V. Demontis, F. Rossella,A. Fontana,S. Cornia, I. Cristiani, *Polarization Control in Integrated Silicon Waveguides Using Semiconductor Nanowires*, Nanomaterials vol. 12(14), 2438, 2022.

[10] A. K. Zvezdin and V. A. Kotov, *Modern Magnetooptics and Magnetooptical Materials, CRC Press*, London, 1997.

[11] P. S. Pershan, *Magneto-Optical Effects,* Journal of Applied Physics 38(3), pp.1482-1490, 1967.

[12] K. Ando, *Magneto-Optics*, Springer Series in Solid-State Sciences Vol. 128, Springer, 2000.

[13] F. Tambag, K. Koksal, H. F. Yildiz, and M. Babiker, *Direct observation of the Faraday rotation using radially-polarised doughnut modes*, Optics Communications vol. 545, 2023.

[14] N. Daloi, T. N. Dey, *Vector Beam Polarization Rotation Control Using Resonant Magneto Optics,* Optics Express 30(12), p. 21894, 2022.

[15] Y. Zhang, C. Yang, S. Li, H. Yan, J. Yin, C. Gu, G. Jin, *Complete Polarization Controller Based on Magneto-Optic Crystals and Fixed Quarter Wave Plates*, Optics Express 14(8), p. 3484, 2006.

[16] D. Shahwar, H. H. Yoon, S. T. Akkanen, D. Li, S. T. Muntaha, M. Cherchi, Z. Sun, *Polarization Management in Silicon Photonics*, npj Nanophotonics 1, 2024.

[17] G. Chen, B. Wu, Q. Wang, F. Wen, and K. Qiu, *Magneto-Optical Fiber-Based Orbital Angular Momentum Mode Converters*, Applied Optics 63, p. 2469, 2024.

[18] N. Li, Y. Chen, C. Zhang, J. Nong, W. Xu, Z. Wang, and Z. Zhang, *Characterization of Fiber-Optic Vector Magnetic Field Sensors Based on the Magneto-Strictive Effect,* Sensors 23, 7127,2023.

[19] G. Armelles, A. Cebollada, A. Garc´ıa-Mart´ın, and M. U. Gonz´alez, *Magnetoplasmonics: Combining Magnetic and Plasmonic Functionalities*, Advanced Optical Materials 1, p.10, 2013.

[20] Z. Bomzon, V. Kleiner, and E. Hasman, *Space-Variant Pancharatnam–Berry Phase Optical Elements with Computer-Generated Subwavelength Gratings*, Optics Letters 27, p. 1141, 2002.